



Journal of Applied Research and Technology

ISSN: 1665-6423

[jart@aleph.cinstrum.unam.mx](mailto:jart@aleph.cinstrum.unam.mx)

Centro de Ciencias Aplicadas y Desarrollo

Tecnológico

México

Hernández-Martínez, A.R.; Estevez, M.; Vargas, S.; Quintanilla, F.; Rodríguez, R.

Natural Pigment-Based Dye-Sensitized Solar Cells

Journal of Applied Research and Technology, vol. 10, núm. 1, 2012, pp. 38-47

Centro de Ciencias Aplicadas y Desarrollo Tecnológico

Distrito Federal, México

Available in: <http://www.redalyc.org/articulo.oa?id=47423226005>

- How to cite
- Complete issue
- More information about this article
- Journal's homepage in [redalyc.org](http://redalyc.org)

[redalyc.org](http://redalyc.org)

Scientific Information System

Network of Scientific Journals from Latin America, the Caribbean, Spain and Portugal

Non-profit academic project, developed under the open access initiative

## Natural Pigment-Based Dye-Sensitized Solar Cells

A.R. Hernández-Martínez<sup>\*1</sup>, M. Estevez<sup>2</sup>, S. Vargas<sup>3</sup>, F. Quintanilla<sup>4</sup>, R. Rodríguez<sup>5</sup>

<sup>1,2,3,5</sup> Centro de Física Aplicada y Tecnología Avanzada  
Universidad Nacional Autónoma de México, Campus Juriquilla  
Boulevard Juriquilla No. 3001, C.P. 76230, Juriquilla, Qro. Mexico  
<sup>\*</sup>ahm@fata.unam.mx

<sup>4,5</sup> Ciencias de la Salud Universidad del Valle de México,  
Campus Querétaro Blvd. Villas del Mesón No. 1000,  
CP 76230, Juriquilla, Qro. Mexico

1<sup>ST</sup> INTERNATIONAL  
CONGRESS ON  
INSTRUMENTATION AND  
APPLIED SCIENCES

### ABSTRACT

The performance of dye-sensitized solar cells (DSSC) based on natural dyes extracted from five different sources is reported. These are inexpensive, have no nutritional use, and are easy to find in Mexico. The solar cells were assembled using a thin film and a TiO<sub>2</sub> mesoporous film on ITO-coated glass; these films were characterized by FTIR. The extracts were characterized using UV-Vis and typical I-V curves were obtained for the cells. The best performance was for *Punica Granatum* with a solar energy conversion efficiency of 1.86%, with a current density J<sub>sc</sub> of 3.341 mA/cm<sup>2</sup> using an incident irradiation of 100 mW/cm<sup>2</sup> at 25 °C.

Keywords: Dye-sensitized solar cells, betalain, natural dyes, solar energy, dip coating.

### RESUMEN

Se reporta en este informe el rendimiento de las celdas solares sensibilizadas por colorante (DSSC) basado en un tinte natural extraído de cinco diferentes fuentes que no tienen usos nutricionales, que son de bajo costo y de fácil adquisición en México. Las celdas solares se construyeron con una película delgada y otra mesoporosa de TiO<sub>2</sub> sobre un vidrio recubierto de ITO; estas películas se caracterizaron mediante FTIR. Los extractos se caracterizaron utilizando espectrometría UV-Vis y la típica curva I-V. El mayor rendimiento fue encontrado en el extracto de *Punica Granatum* con una eficiencia de conversión de energía solar de 1,86%, con una densidad de corriente J<sub>sc</sub> de 3.341 mA/cm<sup>2</sup> con una irradiación de 100 mW/cm<sup>2</sup> a 25 °C.

### 1. Introduction

Dye-sensitized solar cells (DSSCs) are a new type of solar cells developed by Grätzel et al [1]. These are composed of nanocrystalline porous semiconductor electrode-absorbed dye, a counter electrode, and an electrolyte of iodide-triiodide ions. DSSCs are based on the photosensitization produced by the dyes on wide band-gap mesoporous metal oxide semiconductors; this sensitization is due to the dye absorption of part of the visible light spectrum [2, 3]. In this sense, the sensitized dye plays an input role in absorbing sunlight and transforming it into electric energy.

Several metal complexes and organic dyes have been synthesized and used as sensitizers including porphyrins [4], phthalocyanines [5, 6], platinum complexes [7], fluorescent dyes [8], among others.

Ru-based complexes sensitizers have been widely used because they have better efficiency and high durability. However, these advantages are offset by their high cost, their complicated synthetic routes and the tendency to undergo degradation in presence of water [9].

The use of natural pigments as sensitizing dye for the conversion of solar energy in electricity is interesting because, on one hand it enhances the economical aspect and, on the other, it has significant benefits from the environmental point of view [10, 11]. Natural pigments extracted from fruits and vegetables [12-14], such as chlorophyll and anthocyanins, have been extensively investigated as sensitizers for DSSCs. Recently Calogero et al. reported that a conversion efficiency of 0.66% was

obtained using red Sicilian orange juice dye as sensitizer [14]. Wongcharee et al. employed rosella as sensitizer which achieved a conversion efficiency of 0.70% [15]. Roy et al. indicated that using Rose Bengal dye resulted in 2.09% conversion efficiency [16]. Wang et al. used the Coumarin derivation dye as sensitizer with an efficiency of 7.6% [17 – 20].

In this paper, we report the performance of 5 natural dyes extracted from *Festuca ovina*, *Hibiscus sabdariffa*, *Tagetes erecta*, *Bougainvillea spectabilis*, and *Punica granatum* peel; these sources have no nutritional use hence their use poses no conflict related to the issue of energy production; additionally, they are inexpensive and easy to find in Mexico.

## 2. Experimental

### 2.1 Preparation of Dye-Sensitizer Solutions

All dye sources were harvested in central Mexico (Queretaro), grounded in a mortar to obtain a fine powder and dried to reach constant weight at 40 °C. 20 g of each of these powders were placed in amber glass bottles of 40 mL and filled with methanol; these solutions were kept for one week at room temperature and in dark conditions. The extracts were filtered and centrifuged separately to remove any solid residue and stabilized at pH = 4.0 by the addition of an aqueous solution 1N of HCl. The dye solutions were stored in the dark and refrigerated at 4 °C [21].

### 2.2 Electrodes Preparation

The conductive glass plates were ITO-coated glass slides ( $\text{In}_2\text{O}_3\cdot\text{SnO}_2$ ) with a sheet resistance of 30-60  $\Omega/\text{cm}^2$ , 84% transmittance nominal at 550 nm, dimensions (L,W,D) of 25 x 25 x 1.1 mm. Titanium oxide ( $\text{TiO}_2$ ) nanopowder (mesh 320) (Aldrich) and the solvents, ethanol and acetonitrile (Aldrich), were analytic grade; they were used as received. ITO substrates were ultrasonically cleaned in an ethanol-water mixture for 30 min and then heated at 450 °C for 30 min prior to film deposition. The photo-anodes were prepared by depositing two  $\text{TiO}_2$  films on the cleaned ITO glass: for the first one, the ITO glass was immersed in a sol-gel solution containing a mixture of titanium isopropoxide, water and isopropanol at

concentration 2:1:25 vol; the immersion was at constant speed (1.5 cm/min) [22]; the coated glass was heated at 450 °C for 30 min producing a densified  $\text{TiO}_2$  thin film; this isolates the dye-activated porous  $\text{TiO}_2$  layer from the conductor glass. Subsequently, two opposite edges of the ITO glass plate were covered with adhesive tape (Scotch 3M) to control the thickness of the film; finally, a  $\text{TiO}_2$  paste was spread uniformly on the substrate by sliding a glass rod along the tape spacer. The  $\text{TiO}_2$  paste was prepared by mixing 3.0 g of  $\text{TiO}_2$  nano-powder, 10 mL of nitric acid 0.1 N and 4 mL of polyethylene glycol; this suspension was stirred in a closed glass container for 24 hours to obtain a smooth paste with the appropriate viscosity. The film was heated at 450 °C for 60 minutes resulting in a mesoporous opaque film with a thickness of around 8–10  $\mu\text{m}$ . The  $\text{TiO}_2$  photo-anodes were first soaked for 12 h in HCl and then immersed in the natural dye solutions for one night at room temperature, according to published procedures [9]. Later, the photo-anodes were rinsed with distilled water and ethanol and dried. Carbon coated counter electrodes were prepared following a procedure reported elsewhere [23].

### 2.3 DSSC Assembling

An electrolyte solution was prepared as reported elsewhere [9]: 0.1 M of I<sub>2</sub> was mixed with 0.05 M of LiI and 0.05 M of 3-methoxypropionitrile in 50 mL of acetonitrile ( $\text{C}_2\text{H}_3\text{N}$ ) and stirring for 60 minutes. This electrolyte solution was poured in the mesoporous  $\text{TiO}_2$  film which was previously prepared using paraffin-film as framework to seal the cells against an acid attack. The counter electrode was pressed against the impregnated anode and clamped firmly in a sandwich configuration. No leaks (solvent evaporation) were detected.

### 2.4 Characterization

The topology of the  $\text{TiO}_2$  films was obtained using a scanning electron microscope (SEM) Jeol JSM-6060LV operated at 20 kV in secondary electron mode with different magnifications; the samples were previously covered with a gold film. The particle size and the particle size distribution of the commercial  $\text{TiO}_2$  particles were determined using a light scattering apparatus Brookhaven Instruments model BI200SM, equipped with a high speed

digital correlator PCI-BI9000AT, a solid-state photon detector and a He-Ne laser of 35 mW Melles Griot 9167EB-1 as a light source. The crystalline structure of the  $\text{TiO}_2$  thin film was determined using a diffractometer Rigaku model Miniflex+ equipped with a radiation source of 1.54 Å and the angle  $2\theta$  was varied from  $5^\circ$  to  $80^\circ$  at a scan of  $2^\circ/\text{min}$ . FTIR and  $\square$ -Ramman spectra of the initial and the modified ITO-glass substrate were obtained using a FT-IR Sentra Bruker spectrometer and a  $\square$  Ramman Nicolet spectrometer model 910. Absorption spectra were obtained using a UV-Vis spectrometer Genesys 2PC. The DSSCs were illuminated using a 300 W Halogen lamp with an incident power of about  $100 \text{ mW}/\text{cm}^2$ , in an illumination area of  $0.96 \text{ cm}^2$ ; UV and IR filter glasses were used in front of the sample. Photocurrent and photovoltage were measured using a Keithley 2400 source meter and

the incident light power was determined using a Powermeter Thor Labs S130A (0-300 mW) and a Spectrometer Ocean Optics HR 400.

### 3. Results and discussion

#### 3.1 Absorption Spectra

Figures 1 and 2 show the absorption spectra in the region from 250 to 450 nm and the absorption spectra in the region from 450 to 700, respectively, for the five extracts diluted in methanol. In the case of *Festuca ovina*, one region of maximum absorbance was found in the blue close to 420 nm and other in the red close to 660 nm; this is consistent with the peaks of maximum absorbance of chlorophyll A [24]. However, due to weak definition in both regions, the existence of a mixture of chlorophyll B should be inferred, with a higher proportion of chlorophyll A.

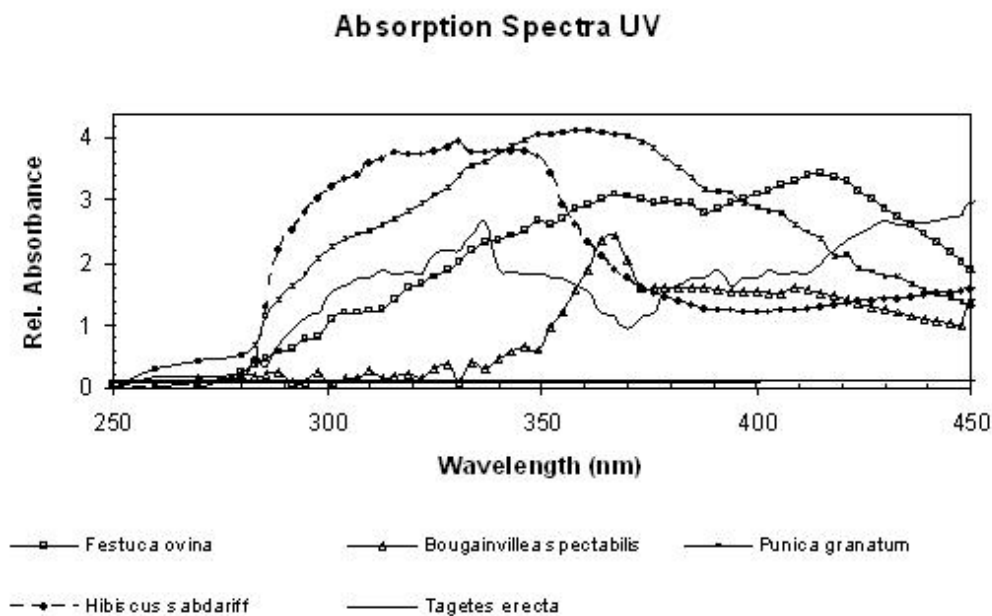


Figure 1. Absorption spectra in methanol between 250 to 450 nm and at pH = 4.

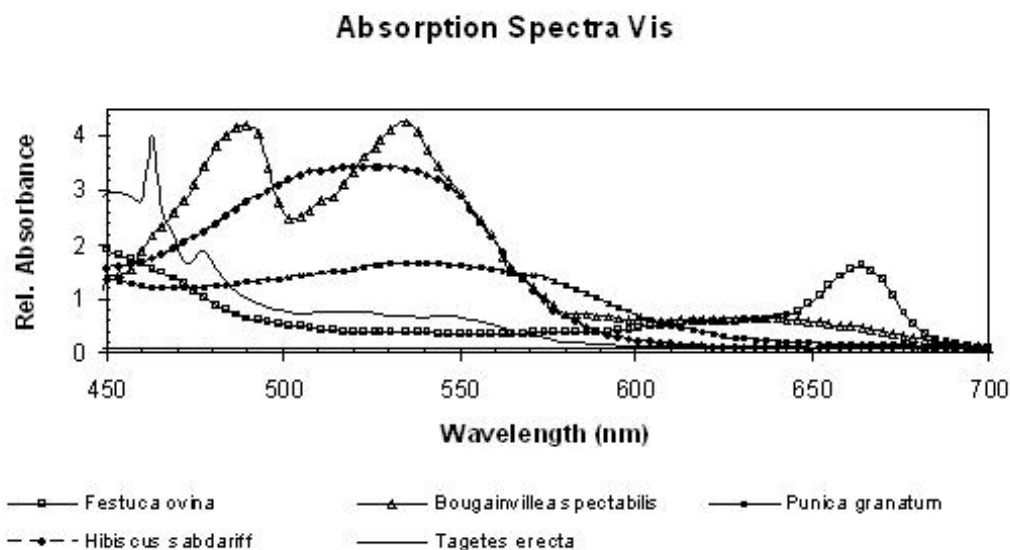


Figure 2. Absorption spectra in methanol between 450 to 700 nm and at pH = 4.

A similar case happens with *Punica granatum* in which a maximum absorbance region was found in the range from 300 to 400 nm corresponding to a mixture of anthocyanins [25].

For the case of *Hibiscus sabdariffa*, Figures 1 and 2 show the typical absorption spectra obtained by Enrico Prenesti et al. for *Hibiscus sabdariffa* flowers at pH 4 that corresponds to a mixture of anthocyanins [26].

For *Tagetes erecta*, the absorption spectrum indicates the presence of lutein in the group of the xanthophylls with characteristic peaks between 300 to 350 and between 450 to 500 [27].

For *Bougainvillea*, two peaks were found: the first one around 480 nm and the second one at 535 nm; they are attributable to the betanin or the bougainvillein-r [28].

### 3.1 IR and Raman Spectra

In Figures 3a through 3c, the IR absorption spectra of TiO<sub>2</sub> films are shown; the ITO conductor glass presents two peaks (Figure 3a) at 770 and 915 cm<sup>-1</sup>. Figure 3b shows the spectrum of the TiO<sub>2</sub> film on the ITO conductor glass where it is possible to see the ITO characteristic peaks at 757 and 923 cm<sup>-1</sup>; these bands mask the characteristic peak of TiO<sub>2</sub> (700 cm<sup>-1</sup>). However, this figure shows a significant change in the chemical structure as evidenced by the shift of the first peak from 770 to 757 cm<sup>-1</sup> (approaching to the TiO<sub>2</sub> typical peak at 700 cm<sup>-1</sup>).

Figure 3c shows the IR spectrum of the conductor glass with two layers of TiO<sub>2</sub>. Due to the higher concentration of TiO<sub>2</sub> present in the sample, a small peak near 770 cm<sup>-1</sup> and two characteristic peaks (757 and 954 cm<sup>-1</sup>) of conductor glass were obtained; a third peak around 1584 cm<sup>-1</sup> was associated mainly to the presence of moisture within the TiO<sub>2</sub>.

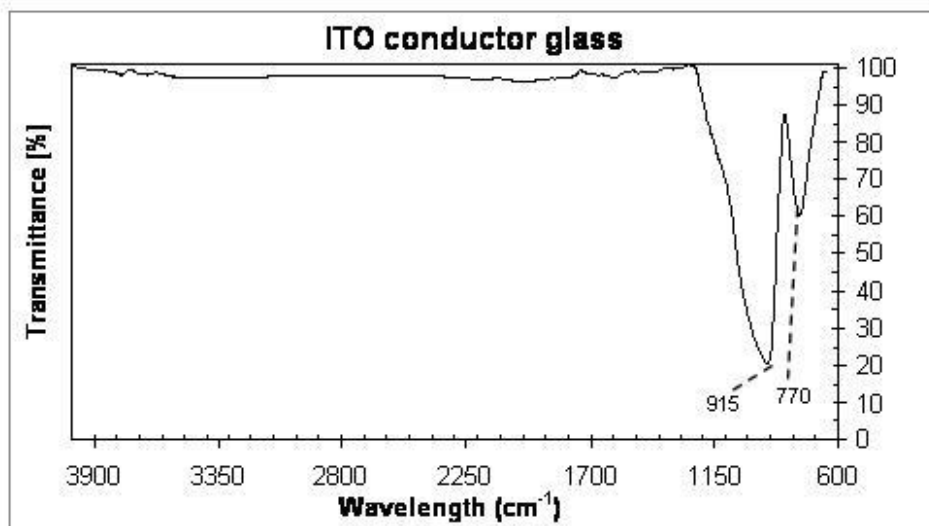


Figure 3a. IR spectra of conductive ITO-coated glass slide.

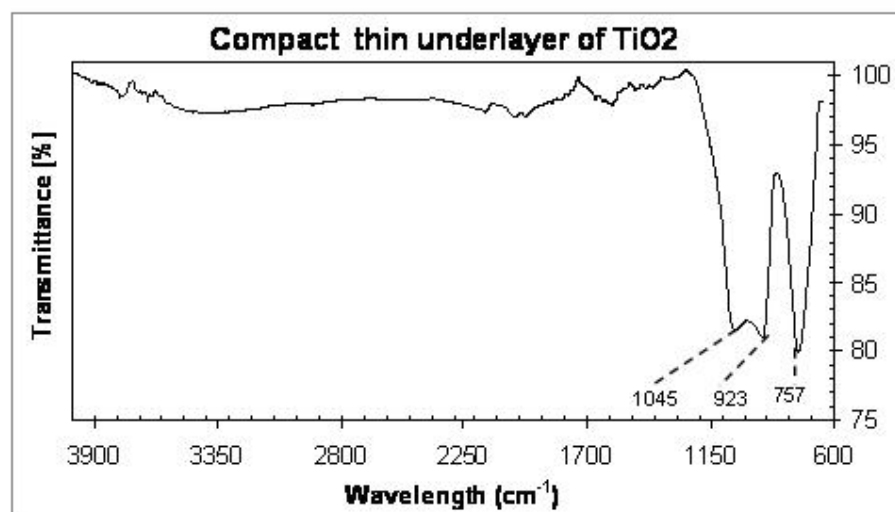


Figure 3b. IR spectra of TiO<sub>2</sub> compact layer overlying the conductive glass plates.

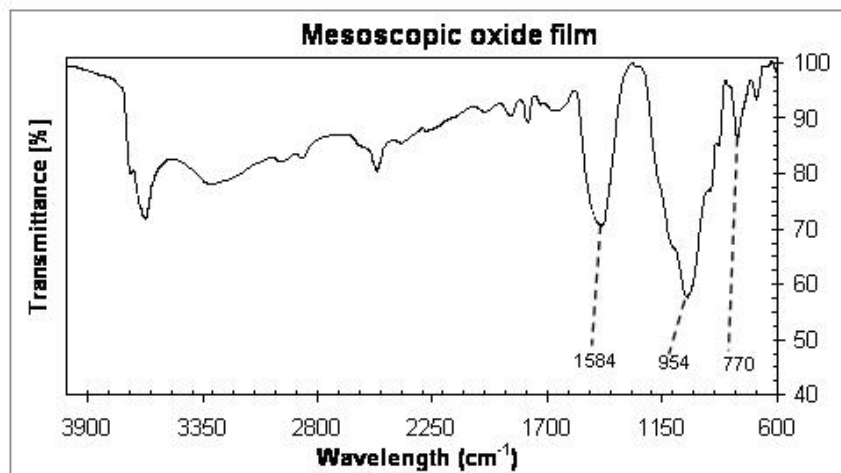


Figure 3c. IR spectra of ITO glass conductor plates with two layers of  $\text{TiO}_2$ .

### 3.3 Structure and Surface Characteristic.

The particle size and the particle size distribution of the commercial  $\text{TiO}_2$  particles were determined by DLS resulting on  $(285 \pm 15)$  nm. The  $\text{TiO}_2$  surface morphology is shown in Figures 4a and 4b. Figure 4a shows a compact (no pore) structure of the first of  $\text{TiO}_2$  thin layer obtained by immersing the ITO plates into a titanium alkoxide sol-gel precursor. This thin film acts as an insulator between the ITO layer and the dye-activated

porous  $\text{TiO}_2$  layer. Some authors [12] have proved the usefulness of the compact layer to achieve a higher efficiency in the performance of the DSSC. On the other side, Figure 4b shows the surface of the thick  $\text{TiO}_2$  coating obtained by the screen-printing technique; here it is possible to see a homogeneous mesoporous surface formed by the  $\text{TiO}_2$  nanoparticles. The nanoporous structure is useful because it has a high effective surface area where the molecules of the extracts can be linked.

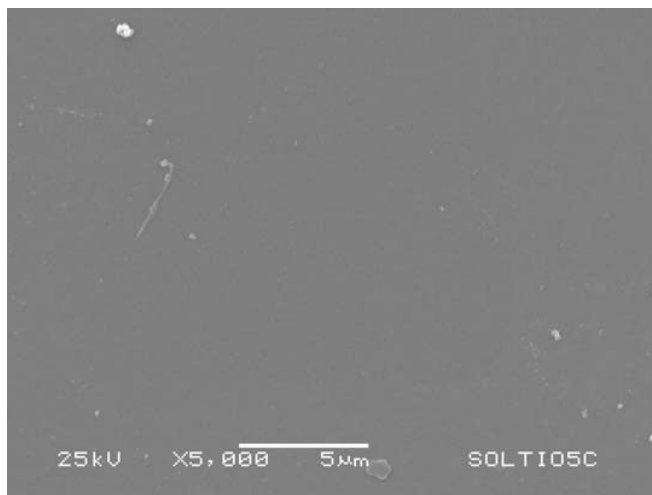


Figure 4a. SEM images of  $\text{TiO}_2$  compact layer overlying conductive glass plates.

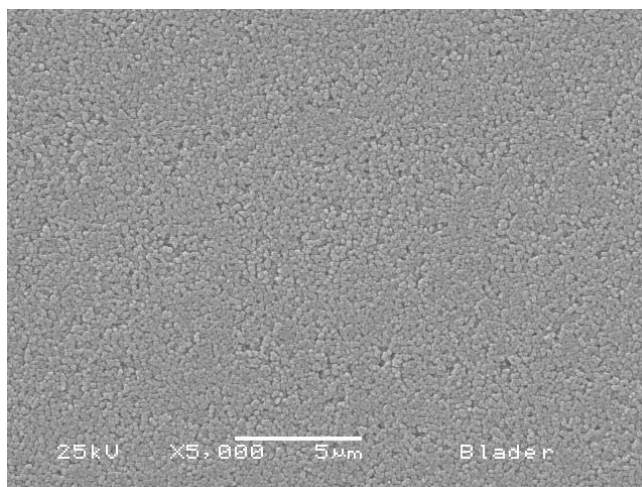


Figure 4b. SEM images of the second nanoporous TiO<sub>2</sub> layer formed by screen-printing technique.

### 3.4 Photoelectrochemistry

Photovoltaic tests of DSSCs using five different extracts from natural sources as sensitizers were performed by measuring the current–voltage (I–V) curves under irradiation with white light (100 mWcm<sup>-2</sup>) from a 300 W halogen lamp. The performance of natural dyes as sensitizers in DSSCs was evaluated by short circuit current

(J<sub>sc</sub>), open circuit voltage (V<sub>oc</sub>), current density at maximum power (J<sub>MP</sub>), maximum power voltage (V<sub>MP</sub>), maximum power (P<sub>M</sub>), theoretical power (P<sub>T</sub>), fill factor (FF), and energy conversion efficiency (η). The photoelectrochemical parameters of the DSSCs sensitized with *Festuca ovina*, *Hibiscus sabdariffa*, *Tagetes erecta*, *Bougainvillea spectabilis*, and *Punica granatum* peel dyes are listed in Table 1.

Dye Source	J <sub>sc</sub> (mA/cm <sup>2</sup> )	J <sub>MP</sub> (mA/cm <sup>2</sup> )	V <sub>OC</sub> (V)	V <sub>MP</sub> (V)	P <sub>M</sub> (mW)	P <sub>T</sub> (mW)	FF	η (%)
<i>Festuca ovina</i>	1.189	0.99	0.548	0.46	0.4554	0.65	0.699	0.46
<i>Hibiscus sabdariffa</i>	3.549	3.2	0.66	0.5	1.6	2.34	0.683	1.6
<i>Tagetes erecta</i>	2.891	2.6	0.475	0.32	0.832	1.37	0.606	0.8
<i>Bougainvillea spectabilis</i>	2.344	1.966	0.26	0.231	0.45	0.61	0.738	0.46
<i>Punica granatum</i> peel	3.341	3.2	0.716	0.58	1.856	2.39	0.776	1.86

Table 1. Electrical characterization of all prepared cells.



The photoelectrochemical parameters were obtained from Figures 5 and 6. Figure 5 shows the typical I–V curves of the DSSCs using the sensitizers extracted from *Festuca ovina*, *Hibiscus sabdariffa*, *Tagetes erecta*, *Bougainvillea spectabilis* and *Punica granatum* peel; the photopower curves are shown in Figure 6.

*Hibiscus sabdariffa* and *Punica granatum* extracts have the best performance parameters, both extracts corresponding to anthocyanins, because the chemical adsorption of these dyes occurs due to the condensation of alcoholic-bound protons with the hydroxyl groups on the surface of nanostructured TiO<sub>2</sub> [29].

*Tagetes erecta* also had good photoelectrochemical parameters due to the

presence of lutein, which also contains hydroxyl groups but a lesser amount of anthocyanins. On the other hand, *Bougainvillea* extracts contain betaxanthin and betacyanins, each one with absorptions at different wavelengths, helping the cell to capture photons of two different energies Zhang [9], meaning that it has acceptable photochemical parameters.

This four extracts displayed interesting photoelectrochemical performance parameters because they are helped by the electrolyte composed of 0.1 M I<sub>2</sub>/0.05 M LiI/0.05 M 3-methoxypropionitrile in acetonitrile (C<sub>2</sub>H<sub>3</sub>N); in addition to this, there is the presence of a compact TiO<sub>2</sub> under-layer (i.e. the overcrowding layer).

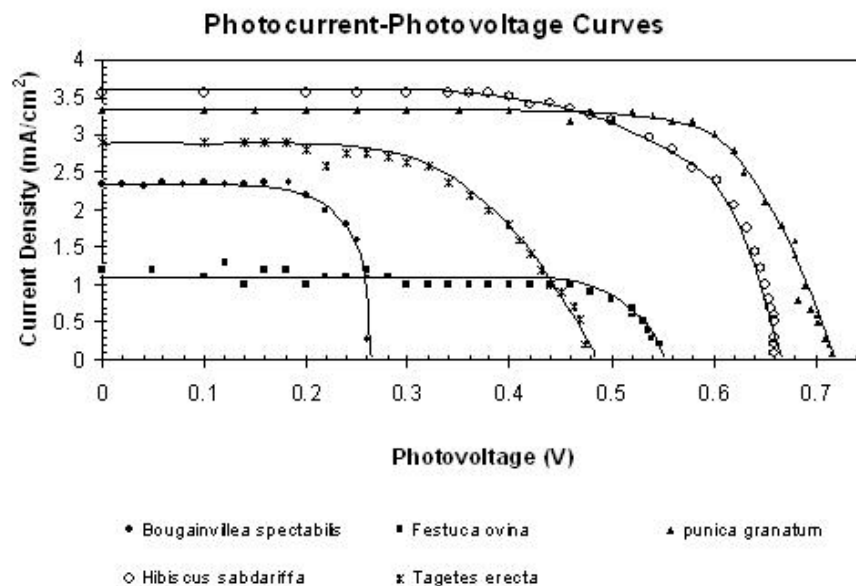


Figure 5. Photocurrent-photovoltage curves for the five extracts sensitized solar cell.

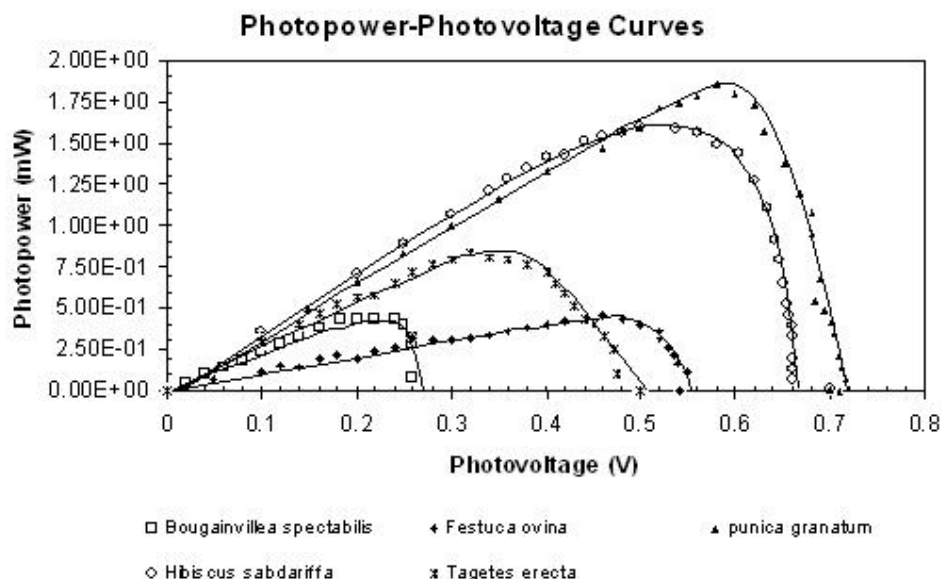


Figure 6. Power- Power-photovoltage curves for the five extracts sensitized solar cell.

## Conclusions

The *Festuca ovina*, *Hibiscus sabdariffa*, *Tagetes erecta*, *Bougainvillea spectabilis* and *Punica granatum* extracts were studied as natural dyes for DSSCs. Some of the results are consistent with those reported previously; however, a higher FF was obtained due to the presence of the insulating TiO<sub>2</sub> layer; this being an important parameter in the evaluation of the solar cell performance because it is the ratio of the maximum obtainable power to the theoretical power. One important finding was that the mixture of betaxanthin and betacyanin produce solar cells with good performance because the absorption at different wavelengths of betaxanthin and betacyanin increases the absorption of photons of different energies. The presence of the hydroxyl group was found to favor the chemical adsorption of these dyes on the surface of TiO<sub>2</sub> improving the electron transfer. It is important to characterize previously the extract from different sources in order to find the best efficiency and the low cost.

## References

- [1] O'Regan, M. Grätzel, Nature 353 (1991), 737–740
- [2] M. Grätzel, Inorg. Chem. 44 (2005) 6841 – 6851.
- [3] N.M. Gómez-Ortiz, I.A. Vázquez-Maldonado, A.R. Pérez-Espadas, G.J. Mena-Rejón, J.A. Azamar-Barrios, G. Oskam, Solar Energy Mater. Solar Cells 94 (2010) 40 – 44.
- [4] F. Odobel, E. Blart, M. Lagrée, J. Mat. Chem., 13, 3, (2003) 502–510.
- [5] MD. K. Nazeeruddin, R. Humphry-Baker, M. Grätzel, D. Wörle, G. Schnurpfeil, G. Schneider, A. Hirth, N. Trombach, J. Porphyrins and Phthalocyanines, 3 (1999) 230–237.
- [6] J. He, A. Hagfeldt, S. E. Lindquist, Langmuir, 17 (2001) 2743–2747.
- [7] A. Islam, H. Sugihara, K. Hara, L. P. Singh, R. Katoh, M. Yanagida, Y. Takahashi, S. Murata, H. Arakawa, Inorg. Chem., 40 (2001) 5371–5380.

- [8] J. M. Rehm, G. L. McLendon, Y. Nagasawa, K. Yoshihara, J. Moser, and M. Grätzel, *J. Phys. Chem.*, 100, 23, (1996) 9577–9588.
- [9] D. Zhang, S.M. Lanier, J.A. Downing, J.L. Avent, J. Lum, J.L. McHale, *Photochem. Photobiol. A: Chem.* 195 (2008) 72–80.
- [10] A. Kay and M. Graetzel, *J. Phys. Chem.*, 97, 23, (1993) 6272–6277.
- [11] M. K. Nazeeruddin, A. Kay, I. Rodicio, J. Amer. Chem. Soc., 115, 14 (1993) 6382–6390.
- [12] G. Calogero, G. D. Marco, S. Cazzanti, S. Caramori, R. Argazzi, A. D. Carlo, C. A. Bignozzi, *Int. J. Mol. Sci.*, 11 (2010) 254–267.
- [13] C.G. Garcia, A. S. Polo, and N. Y. Murakami Iha, *J. Photochem. Photobiol. A*, 160, (2003) 87–91.
- [14] G. Calogero G. D. Marco, *Energ. Mat. Sol. C*, 92, (2008), 1341–1346.
- [15] K. Wongcharee, V. Meeyoo, S. Chavadej, *Sol. Energ. Mat. Sol. C* 91 (2007) 566–571.
- [16] M.S. Roy, P. Balraju, M. Kumar, G.D. Sharma, *Sol. Energ. Mat. Sol. C* 92 (2008) 909–913.
- [17] Z.-S. Wang, K. Hara, Y. Dan-oh, C. Kasada, A. Shinpo, S. Suga, H. Arakawa, H. Sugihara, *J. Phys. Chem. B* 109 (2005) 3907–3914.
- [18] Z.-S. Wang, Y. Cui, K. Hara, Y. Dan-oh, C. Kasada, A. Shinpo, *Adv. Mater.* 19 (2007) 1138–1141.
- [19] Z.-S. Wang, Y. Cui, Y. Dan-oh, C. Kasada, A. Shinpo, K. Hara, *J. Phys. Chem. C* 111 (2007) 7224–7230.
- [20] Z.-S. Wang, Y. Cui, Y. Dan-oh, C. Kasada, A. Shinpo, K. Hara, *J. Phys. Chem. C* 112 (2008) 17011–17017.
- [21] R.Castellar, J.M.Obon, M. Alacid, J.A Fernandez-lopez, *J. Agric. Food Chem.*, 51 (2003) 2772–2776.
- [22] C. Su, T.K. Sheu, Y.T Chang, M.A Wan, M.C Feng, W.C Hung, *Synthetic Metals* 153 (2005) 9-12
- [23] Greg P. Smestad, *Solar Ener. Mat. Solar Cells*, 55 (1998) 157–178.
- [24] Hartmut K. Lichtenthaler, Claus Buschmann, *Current Protocols in Food Analytical Chemistry* UNIT F4.3, 2001.
- [25] M.Mónica Giusti, Ronald E. Wrolstad, *Current Protocols in Food Analytical Chemistry* UNIT F1.2, 2001.
- [26] Enrico Prenesti, Silvia Berto, Pier G. Daniele, Simona Toso, *Food Chemistry* 100 (2007) 433–438.
- [27] W. Leigh Hadden, Ruth H. Watkins, Luis W. Levy, Edmundo Regalado, Diana M. Rivadeneira, Richard B. van Breemen, Steven J. Schwartz, *J. Agric. Food Chem.* 1999, 47, 4189–4194.
- [28] F.D Sánchez, E.M.S. Lopez, S.F. Kerstupp, R.V. Ibarra, L. Scheinvar, *J. Environ. Agric. Food Chem.*, 5 (2006) 1330–1337.
- [29] S. Meng, J. Ren, E. Kaxiras, *Nano Lett.* 8 (2008) 3266–3272.

#### Acknowledgments

The authors are in debt to A. del Real for the SEM microimages, D. Rangel for instrumental support and G. Hernandez for FTIR and micro-Raman analysis. One of the authors (AHM) is in debt for the economical support from DGAPA, UNAM.